Precision Engineering 37 (2013) 765–770

Contents lists available at SciVerse ScienceDirect

Precision Engineering

journal homepage: www.elsevier.com/locate/precision

Application of large deflection analysis for tool design optimization in an electrochemical curved hole machining method

Mitsuo Uchiyama [a,*], Masanori Kunieda [b]

[a] *Department of Mechanical Engineering, Kanto Gakuin University, 1-50-1 Mutsuurahigashi, Kanazawa-ku, Yokohama-shi, Kanagawa 236-8501, Japan*
[b] *Department of Precision Engineering, The University of Tokyo, 7-3-1 Hongo, Bunkyo-ku, Tokyo 113-8656, Japan*

ARTICLE INFO

Article history:
Received 27 September 2012
Received in revised form 13 February 2013
Accepted 28 February 2013
Available online 13 March 2013

Keywords:
Curved hole
Electrochemical machining
Curvature control
Metal mold
Large deflection analysis

ABSTRACT

This paper describes the optimization of the tool design and structure in an electrochemical curved hole machining method. Curved holes can be machined using a flexible tool which can be curved by the hole being processed by the tool itself. The curvature of the hole can be determined by the tilt angle of the electrode tip attached to the end of the tool. The tool design was optimized by a numerical analysis of the electrostatic field and a large deflection to reduce the radius of curvature and to improve machining efficiency. Machining tests showed that the curved hole shape is controlled by the detailed electrode shape and the feed rate of the electrode. The calculated curved hole shape agreed with the form of the holes machined experimentally.

1. Introduction

Efforts are under way in the automotive industry to integrate component parts for the purpose of lightening the vehicle weight and reducing the part count, which tends to result in larger castings and injection-molded parts. The trend toward these parts has led to the integration of parts that were previously separate components. This has resulted in more complex part shapes and also larger level differences due to recesses and projections. As a result, maintaining the shape accuracy and dimensional accuracy of these parts is continually becoming a more critical issue. The dies and molds used in producing these parts also require more complex shapes, and controlling the die/mold surface temperature has also become an increasingly important issue. In order to control the surface temperature accurately, it is desirable to provide coolant channels in dies/molds at a constant distance from the surface and following the curvatures of the parts to be produced.

One solution to this issue lies in curved hole machining methods and various techniques have been developed over the years [1–5]. However, most of the curved hole machining methods developed so far involve the attachment of an actuator to the tool body for controlling the shape of the tool while machining is performed. These methods therefore require complex mechanisms and high control accuracy, which limits their applicability to the machining of simple curved shapes. Currently, they are not capable of machining the complex shapes typically found in dies/molds. To overcome this situation, we have developed a curved hole machining method capable of producing even intricately shaped holes. With this method, the tool pre-machines a small hole in the intended machining direction and then follows the hole it has to cut. These operations are repeated in the process of machining a curved hole. Our previous reports [6–8] have presented the results of machining tests conducted with an electrochemical machining method based on this concept. The results confirmed that curved hole machining can be performed with a high degree of freedom that allows the direction and curvature of the curved hole to be varied as the machining process proceeds.

Furthermore, a numerical analysis of the electrostatic field was conducted with the aim of optimizing the design of the electrode shape by examining the characteristics of various electrode shapes. The results of the electrostatic field analysis and actual shapes of machined holes were then compared for the electrodes examined. After optimizing the electrode shape and the machining conditions, an attempt was made to machine actual curved holes.

In the present study, an analysis of large beam deflection was added to the electric field analysis described in our previous reports, thereby making it possible to predict the curved hole shape. Additionally, the relationship between the shapes and dimensions of different parts of the electrode and the resultant curved hole shape was investigated. The overall electrode shape and machining conditions were optimized by making a comparison with the shapes of actual curved holes.

* Corresponding author. Tel.: +81 457867116.
E-mail address: uchiyama@kanto-gakuin.ac.jp (M. Uchiyama).

0141-6359/$ – see front matter © 2013 Elsevier Inc. All rights reserved.
http://dx.doi.org/10.1016/j.precisioneng.2013.03.003

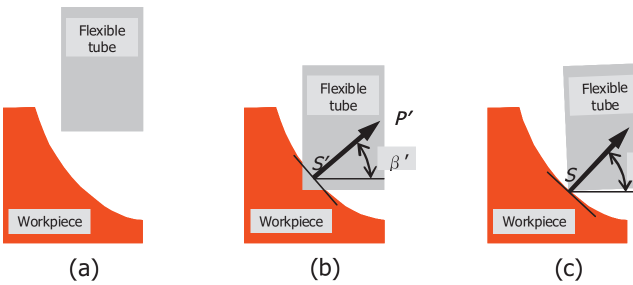

Fig. 1. Contact position and reaction force angle.

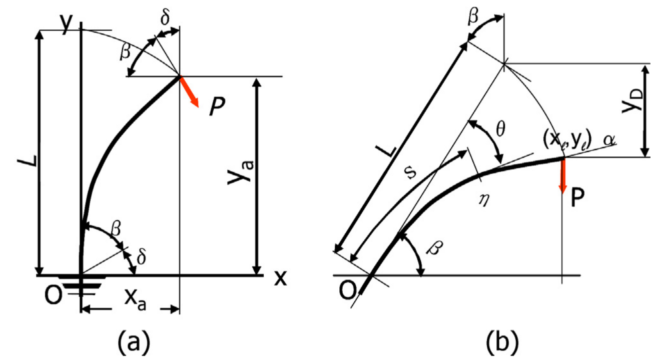

Fig. 2. Deflection curve of flexible tube.

2. Analysis of flexible tube deflection

2.1. Differential equation of large deflection

As the electrode moves along the workpiece surface, it receives reaction force from the workpiece at the point of contact between them, which induces deflection in the flexible tube. Because the magnitude of this deflection is larger than that treated in a linear analysis, it is necessary to analyze the tube shape using the large deflection theory. Based on the position and orientation of the electrode following displacement, the distribution of the amount of stock removed from the workpiece surface is found. The curved hole shape can be analyzed by performing coupled calculations of the deflection amount in a large deflection analysis and the stock removal amount in an electrostatic field analysis.

Fig. 1 shows the positional relationship between the electrode and the workpiece. Fig. 1(a) shows the state where there is no contact at all between the electrode and the workpiece. In this case, the electrode simply advances downward in the figure at predetermined micro-feed amounts, so no deflection occurs in the flexible tube. Fig. 1(b) shows a state in the analysis where the electrode cuts into the workpiece as a result of advancing further. This is a positional relationship that cannot actually occur.

Here, we will let S' denote the center point of the area where the electrode cuts into the workpiece surface. From point S', we draw a line normal to the workpiece surface, forming angle β' with the horizontal. The flexible tube deflects under the reaction force P' received from the workpiece surface in the direction of angle β'. Here, it is assumed that friction is negligibly small. Reaction force P' is increased until the electrode is no longer cutting into the workpiece, thus inducing deflection in the flexible tube until the state is reached where the electrode and the workpiece are in contact, as shown in Fig. 1(c). Here, the position of point S where the electrode and the workpiece are in contact as indicated in Fig. 1(c) differs from point S'. Therefore, it is necessary to repeat the calculations again based on the new angle β. However, that repeated calculation was not performed in this study because the amount the electrode moved in one feed operation was smaller than the size of the analysis patch.

Fig. 2 shows the deflection state of the flexible tube and the applied load considered in the differential equation for large deflection. Fig. 2(a) shows the original state where the load P acts on the tip of the flexible tube as the reaction force from the workpiece at the angle β formed by a line normal to the inclined surface of the workpiece. The fixed end of the flexible tube is held in the vertical direction. Fig. 2(b) shows the state for $\delta = 0^\circ$. It will be noted that the deflection curve in both cases does not change because Fig. 2(a) merely rotates the curve in Fig. 2(b) by an amount equal to angle δ. Therefore, Fig. 2(b) is treated as the basic shape and is analyzed as a large deflection problem [9,10]. In the deflection curve, we define the position of the flexible tube tip as (x_l, y_l) and the angle formed by the tangent at this point and the x-axis as the deflection angle α, and let y_D denote the displacement in the y-axis direction from the no-load position.

Letting L denote the entire length of the flexible tube and E its vertical Young's modulus. Letting point η denote a point at a distance s along the length of the flexible tube from the origin 0 and θ denote the deflection angle at point η from the fixed end of the tube, the equation for the curvature of the tube becomes $d\theta/ds$. The differential equation of the deflection curve can be expressed as

$$EI\frac{\mathrm{d}^2\theta}{\mathrm{d}s^2} = -P\cos\ \theta \tag{a}$$

Defining the nondimensionalized load as

$$\mu = \frac{PL^2}{EI}$$

and assuming that

$$\eta = \frac{S}{L}$$

we obtain

$$\frac{d^2\theta}{d\eta^2} = -\mu\cdot\cos\ \theta \tag{b}$$

The coordinates (x, y) of point η from the fixed end of the flexible tube are expressed as

$$\frac{x}{L} = \int_0^{\eta}\cos\ \theta\, d\eta,\quad \frac{y}{L} = \int_0^{\eta}\sin\theta\, d\eta \tag{c}$$

When the nondimensionalized load μ in Eq. (b) is given, solutions are found based on the following conditions at both ends of the tube in Fig. 2(b):

$$\eta = 0 : \theta = -\beta$$

$$\eta = 1 : \frac{d\theta}{d\eta} = 0$$

The state of the large deflection can be made clear by finding θ as a function of η. Since Eq. (b) is nonlinear, it cannot be solved analytically. In order to find the solution by numerical calculation, the Runge–Kutta method was applied here in a trial-and-error process to find the values of $d\theta/d\eta$ that should be given initially so that the value of $d\theta/d\eta$ at $\eta = 1$ becomes exactly zero. Additionally, the deflection angle α can be found by numerical calculation based on the initial values thus found for $d\theta/d\eta$. Then, the coordinates (x_l, y_l) of the free end of the flexible tube in Fig. 2(b) and the deflection angle α can be found from Eq. (c). As a result, the coordinates (x_a, y_a) in Fig. 2(a) and the deflection angle at the free end of the flexible tube can be found, making it possible to find the inclination and position of the flexible tube tip.